Available online at www.sciencedirect.com
SCIENCE DIRECT®
Analytical Biochemistry 332 (2004) 23–31
ANALYTICAL BIOCHEMISTRY
www.elsevier.com/locate/yabio

Direct electrochemistry and electrocatalysis of myoglobin immobilized on a hexagonal mesoporous silica matrix

Zhihui Dai,[a] Xiaoxing Xu,[a,b] and Huangxian Ju[a,*]

[a] *State Key Laboratory of Coordination Chemistry, Department of Chemistry, Institute of Chemical Biology, Nanjing University, Nanjing 210093, China*
[b] *Department of Chemistry, Changshu College of Jiangsu, Changshu 215500, China*

Received 11 December 2003
Available online 6 July 2004

Abstract

The direct electrochemistry of myoglobin (Mb) immobilized on a hexagonal mesoporous silica (HMS)-modified glassy carbon electrode was described. The interaction between Mb and HMS was investigated by using Fourier transfer infrared spectroscopy, nitrogen adsorption isotherm, and cyclic voltammetry. Two couples of redox peaks corresponding to Fe(III) to Fe(II) conversion of the Mb intercalated in the mesopores and adsorbed on the surface of the HMS were observed with the formal potentials of −0.167 and −0.029 V in 0.1 M, pH 7.0, phosphate buffer solution, respectively. The electrode reaction showed a surface-controlled process with one proton transfer. The immobilized Mb displayed good electrocatalytic responses to the reduction of both hydrogen peroxide (H_2O_2) and nitrite (NO_2^-), which were used to develop novel sensors for H_2O_2 and NO_2^-. The apparent Michaelis–Menten constants of the immobilized Mb for H_2O_2 and NO_2^- were 0.065 and 0.72 mM, respectively, showing good affinity. Under optimal conditions, the sensors could be used for the determinations of H_2O_2 ranging from 4.0 to 124 μM and NO_2^- ranging from 8.0 to 216 μM. The detection limits were 6.2×10^{-8} and 8.0×10^{-7} M at 3 σ, respectively. The HMS provided a novel matrix for protein immobilization and the construction of biosensors via the direct electron transfer of immobilized protein.

Keywords: Biosensors; Myoglobin; Hexagonal mesoporous silica; Chemically modified electrode; Direct electron transfer; Hydrogen peroxide; Nitrite

Myoglobin (Mb)[1] is a small heme protein found in muscle cells with a molecular weight of approximately 16,900 and one polypeptide chain. The physiological function of Mb is to store dioxygen and increase the diffusion rate of dioxygen in the cell. Although Mb does not function physiologically as an electron carrier, it undergoes the oxidation and reduction process in the respiratory system. Thus, its electron transfer reactions play essential roles in biological processes. It is an ideal model molecule for the study of electron transfer reactions of heme proteins, biosensing, and electrocatalysis.

The electrochemistry of Mb has been achieved by using mercury electrodes [1], methyl-viologen-modified gold electrodes [2], and ultraclean and hydrophilic indium oxide electrodes [3,4]. The electrochemical behavior is unstable and extremely sensitive to the sample purity and the conditions of the electrode surface [5]. Great efforts have been made to enhance its electron transfer by using mediators, promoters, or some special modified materials [6–15]. Among these, surfactant micelles have been shown to be efficient in promoting the electrochemistry of Mb. Extensive studies on electrochemistry of Mb using various surfactants such as didodecyl dimethyl ammonium bromide, lipids, LB films, etc. [7,8,14,15] demonstrate that the surfactant film can effectively enhance electron transfer between the protein and the electrode. However, the surfactants have drastic effects on the structure of the heme protein, leading to depletion of heme in solution. Such denaturation of the protein possibly depends on the nature of the surfactant

* Corresponding author. Fax: +86-25-83593593.
E-mail address: hxju@nju.edu.cn (H. Ju).

[1] *Abbreviations used*: GCE, glassy carbon electrode; HMS, hexagonal mesoporous silica; HMS/GCE, HMS-modified GCE; Mb, myoglobin; Mb/GCE, Mb-modified GCE; Mb/HMS/GCE, Mb/HMS-modified GCE; PBS, phosphate buffer solution; PVA, polyvinyl alcohol; FTIR, Fourier transfer infrared; HRP, horseradish peroxidase.

0003-2697/$ - see front matter © 2004 Published by Elsevier Inc.
doi:10.1016/j.ab.2004.03.067

[16]. Thus, it is necessary to search for a way to develop a new Mb-modified electrode with well-behaved electrochemistry and good stability.

Recently, a series of inorganic porous materials such as clay [17], montmorillonite [18–20], porous alumina [21], and sol-gel matrix [22] etc. have been shown to be promising as immobilization matrices. They have the advantages of high mechanical, thermal, and chemical stability and good adsorption and penetrability due to their regular structures and appreciable surface areas. In addition, the unique structural and catalytic properties of molecular sieves for structuring an electrochemical/electron transfer environment and resistance to biodegradation have attracted considerable attention [23]. As protein immobilization matrices, molecular sieves can combine with proteins through physical or chemical action. However, these molecular sieves always contain alumina and their porous diameters are usually too small to bring their unique porous roles fully into play. For example, NaY has been used for microporous molecular sieves with silica-alumina molar ratios of 1.5–3 and pore diameter of 0.81 nm [23]. The vacancy of both its pores and its surface can adsorb water easily due to the presence of alumina, which is a disadvantage during the immobilization of proteins. The mesoporous molecular sieves have much larger pore sizes than microporous molecular sieves, which make them attractive candidates as electrode surface modifiers. The larger pore size can result in a more efficient transport of proteins on the modified electrodes. We here use a mesoporous silica material, hexagonal mesoporous silica (HMS), which processes a porous size of nanoscale dimension to make it more suitable for enzyme intercalation and loading. When it is immersed into aqueous solution, the vacancy of the hexagonal mesopores is difficult to be saturated by water due to its hydrophobic surface. Thus, it can be used for the intercalation of protein. This work demonstrates the application of mesoporous silica materials to protein immobilization, direct electron transfer, and biosensing. The interaction between Mb and HMS is characterized with FTIR, N_2 adsorption isotherms, and cyclic voltammetry. The intercalated Mb shows a direct electrochemistry with a formal potential different from that of the adsorbed Mb. The immobilized Mb exhibits a good electrocatalytic behavior with respect to the pseudo peroxidase activity to H_2O_2 reduction and a fast amperometric response to $NaNO_2$. The prepared sensors could be used for the determinations of H_2O_2 and NO_2^-.

Materials and methods

Reagents

Horse heart Mb (No. M-1882, type III) was purchased from Sigma and used as received. H_2O_2 (30% W/V solution) was purchased from Shanghai Biochemical Regent Co. and $NaNO_2$ from Nanjing Chemical Reagent Factory (China). Polyvinyl alcohol (PVA, average degree of polymerization, 1800 ± 100) was purchased from Shanghai Laize Factory of Fine Chemicals. All other chemicals were of analytical grade and used without further purification. PBS (0.1 M) with various pH values was prepared by mixing stock standard solutions of K_2HPO_4 and KH_2PO_4 and adjusting the pH with H_3PO_4 or NaOH. All solutions were prepared with doubly distilled water.

Immobilization of Mb

HMS was prepared following a recipe similar to that reported by Tanev et al. [24]. The specific surface area and pore volume were obtained by the N_2 adsorption data and calculated by the BET method of Barrett et al. [25] and the diameter of the HMS derived from the adsorption branch by the BJH method are listed in Table 1.

HMS (30 mg) was dispersed into 10 ml, 0.1 mM Mb (in pH 7.0 PBS) solution. The mixture was stirred for 3 h to obtain a suspension. Then 100 μl of the obtained suspension was mixed with 5 μl 3% PVA solution of ethanol/water (V:V 1:1) to produce Mb/HMS colloid that was used for the following work.

Electrode modification

The glassy carbon electrodes (GCE; 3 mm in diameter) were polished to a mirrorlike finish with 1.0-, 0.3-, and 0.05-μm alumina slurry (Beuhler) followed by rinsing thoroughly with doubly distilled water. The electrodes were successively sonicated in 1:1 nitric acid, acetone, and doubly distilled water and then allowed to dry at room temperature. The real area of the pretreated GCE was determined by the slope of the plot of the anodic peak current of 1.0 mM $K_3[Fe(CN)_6]$ in 0.1 M KCl vs. the square root of scan rate to be 0.092 cm^2. Mb/HMS colloidal solution (3 μl) was dropped on the pretreated GCE surface and allowed to dry under ambient conditions for 3 h. After the modified electrode was rinsed with doubly distilled water twice or thrice, Mb/HMS/GCE was obtained. When not in use, the electrode was stored in 0.1 M, pH 7.0, PBS at 4 °C.

Table 1
Pore characterization of HMS

A_{BET} (m^2/g)	V_{total} (cm^3/g)	a_0 (nm)	D (nm)	L (nm)
718	0.57	6.54	4.04	2.50

A_{BET}, total specific surface area; V_{total}, total pore volume; a_0, lattice parameter; D, pore parameter; L, wall thickness.

Apparatus and measurements

Cyclic voltammetric and amperometric measurements were performed on a 270 Electrochemistry System (EG&G, USA). All electrochemical experiments were carried out in a cell containing 5.0 ml 0.1 M PBS at room temperature (25 ± 2 °C) using a platinum wire as auxiliary, a saturated calomel electrode as reference, and the Mb/HMS/GCE as working electrodes. All solutions were deoxygenated by bubbling highly pure nitrogen for at least 10 min and maintained under nitrogen atmosphere during the measurements. The amperometric experiments were carried out by applying potentials of -400 mV for H_2O_2 and -1000 mV for $NaNO_2$ on a stirred cell at 25 ± 2 °C. The sensor responses were measured as the difference between total and residual currents. FTIR spectra were obtained on a Nexus 670 (Nicolet) FTIR instrument at room temperature. Nitrogen adsorption isotherms were obtained using an ASAP 2000 instrument (Micromeritics, Norcross, GA, USA). Before adsorption measurements, the samples were degassed for 2 h at 150 °C.

Results and discussion

Interaction between HMS and Mb

The interaction between HMS and Mb could be demonstrated with FTIR spectra and N_2 adsorption isotherms. The IR spectrum of HMS showed three adsorption bands around 1628, 1089, and 805 cm^{-1} (Fig. 1). The peak at 1628 cm^{-1} was attributed to the vibration of adsorbed water and the others were from the frame symmetric and asymmetric flexible vibrations of Si groups in HMS [26]. The adsorption bands of Mb were at 1659 and 1543 cm^{-1}, which were attributed to the amide I and amide II infrared absorbance bands of Mb and could provide detailed information on the secondary structure of the polypeptide chain [27]. The amide I band (1700–1600 cm^{-1}) is caused by C=O stretching vibrations of peptide linkages in the protein backbone. The amide II band (1620–1500 cm^{-1}) results from a combination of N—H bending and C—N stretching. Upon the adsorption of Mb on HMS, the bands corresponding to the amide I and amide II groups were retained, suggesting that the native structure was not destroyed. The band at 1089 cm^{-1} shifted to 1094 cm^{-1} and the band at 805 cm^{-1} disappeared. The shift of frame vibration band to higher frequency was due to the effect of the intercalated Mb enlarging the porous size [28]. This might result from the interaction between Mb and some specific sites on the inner wall of HMS.

Protein could be fixed in the pores of mesoporous materials by simply immersing the mesoporous material in the protein solution [29]. To clarify the effect of Mb on mesoporous materials, the N_2 adsorption isotherms before and after Mb loading were investigated (Fig. 2). The pore volume of HMS decreased upon the immobilization treatment. The pore volume of HMS was 48.5% of that of HMS before Mb loading, indicating that Mb intercalated into the inner wall of HMS [30].

Direct electrochemistry of Mb/HMS-modified electrode

Fig. 3 shows the cyclic voltammograms of different electrodes in 0.1 M, pH 7.0, PBS at 20 mV/s. No redox peak is observed at both GCE and HMS/GCE, so HMS is electroinactive in the potential window. The Mb/GCE shows one reduction peak that corresponds to the irreversible reduction of Mb. The Mb/HMS/GCE exhibits two couples of stable redox peaks that are attributed to the redox of immobilized Mb. The peak currents are much larger than those of Mb/GCE. The anodic and cathodic peak potentials of the first peak are at 44 and -102 mV, respectively. Another couple of peaks are at -132 and -201 mV. The weaker reversibility and the smaller response of Mb/GCE compared to those of Mb/HMS/GCE indicate that the HMS plays an important role in facilitating the

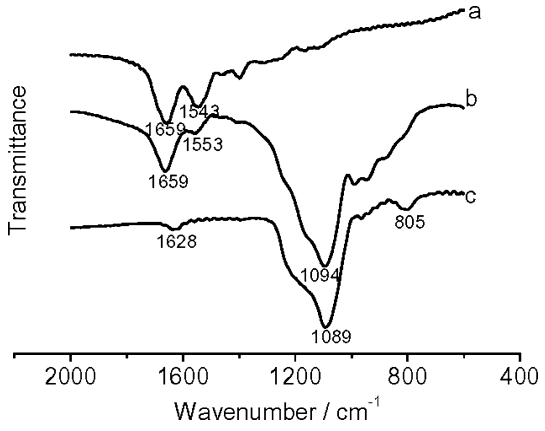

Fig. 1. FTIR spectra of Mb (a), Mb/HMS (b), and HMS (c).

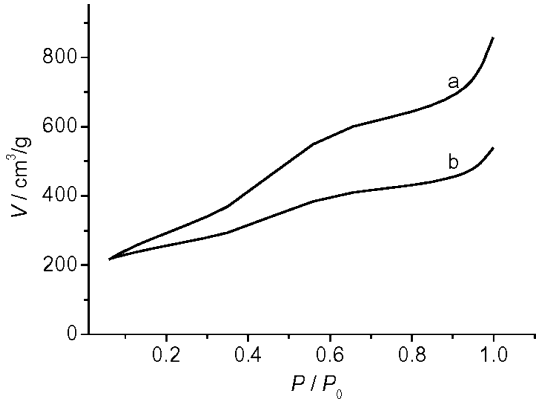

Fig. 2. N_2 adsorption isotherms before (a) and after (b) immobilizing of Mb on HMS.

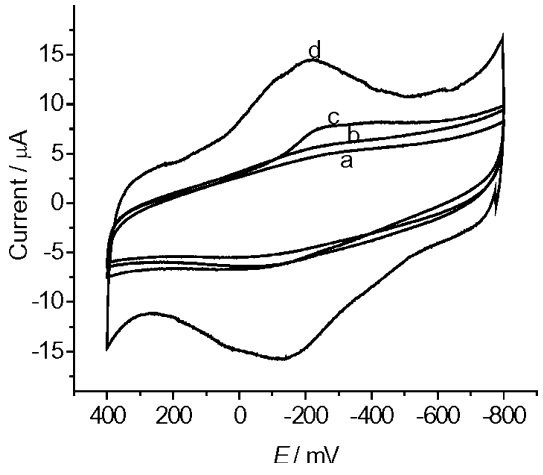

Fig. 3. Cyclic voltammograms on GCE (a), HMS/GCE (b), Mb/GCE (c), and Mb/HMS/GCE (d) in 0.1 M, pH 7.0, PBS at 20 mV/s.

electron exchange between the electroactive center of Mb and the GCE.

The two couples of redox peaks in Fig. 3d corresponded to two states of the immobilized Mb with formal potentials of -0.029 and -0.167 V. The larger total specific area of the pores compared to that of the molecular sieves surface allowed more Mb to intercalate into the pores, thus leading to larger peak currents. The presence of many positive-charged acidic SiOH groups on the surface of HMS [31] made the oxidation of Mb more difficult thermodynamically, resulting in a more positive formal potential of the adsorbed Mb compared to that of the intercalated Mb. Thus, the couple of redox peaks occurring at more negative potentials were attributed to the oxidation and reduction of the Mb immobilized in the inner wall of HMS by the intercalation of Mb in the mesopores of HMS, while the couple of redox peaks occurring at more positive potentials resulted from the oxidation and reduction of the Mb immobilized on the surface of HMS by physical adsorption. The limited space of the mesopores made the reduction of the electroactive center of the intercalated Hb more difficult, resulting in a more negative formal potential.

The effect of scan rate on electrochemistry of the immobilized Mb is shown in Fig. 4. With an increasing scan rate, the anodic peak potential of Mb shifted to a more positive value and the cathodic peak potential shifted in a negative direction. In the scan rate range of 20–180 mV/s, the redox peak currents of the Mb both inside and outside pores increased linearly (insets A and B in Fig. 4), indicating a surface-controlled process [32]. The small peak-to-peak separation indicated a fast electron transfer rate.

The integration of the reduction peaks of Mb/HMS/GCE gave an average total Mb surface coverage of $(4.35 \pm 0.04) \times 10^{-9}$ mol/cm^2. The total coverage was much larger than that of monolayer coverage and those of $(2.72 \pm 0.01) \times 10^{-10}$ mol/cm^2 at Mb/didodecyl dimethyl ammonium polyvinyl sulfate ($2C_{12}N^+PVS^-$) modified electrode [33] and 2.785×10^{-10} mol/cm^2 at Mb/homocysteine/Au electrode [34] due to the very large specific area of the pores of the molecular sieves.

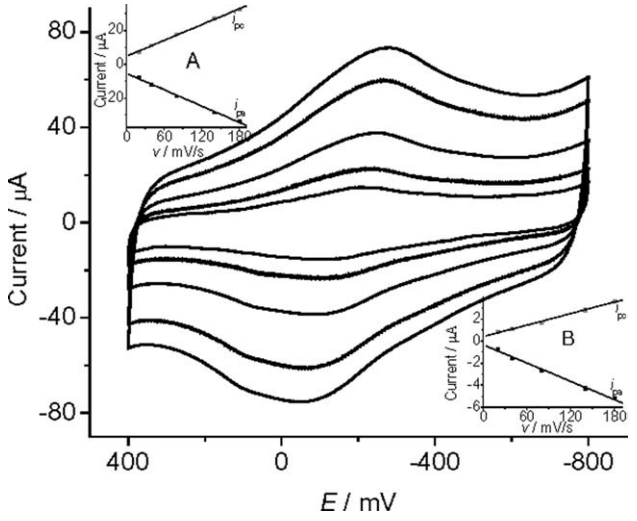

Fig. 4. Cyclic voltammograms of Mb/HMS/GCE in 0.1 M, pH 7.0, PBS at 20, 40, 80, 140, and 180 mV/s (from inner to outer). Inset A: plots of peak currents of intercalated Mb vs v. Inset B: plots of peak currents of adsorbed Mb vs v.

Effect of solution pH on direct electron transfer of Mb

The direct electrochemistry of Mb/HMS/GCE showed a strong dependence on solution pH (Fig. 5). An increase of solution pH caused a negative shift in both cathodic and anodic peak potentials, and the maximum peak currents of Mb occurred at pH 7.0, the isoelectric point of Mb [35]. The same result was also observed for Mb at an indium oxide electrode [3], indicating that the immobilized process did not alter the optimal pH value

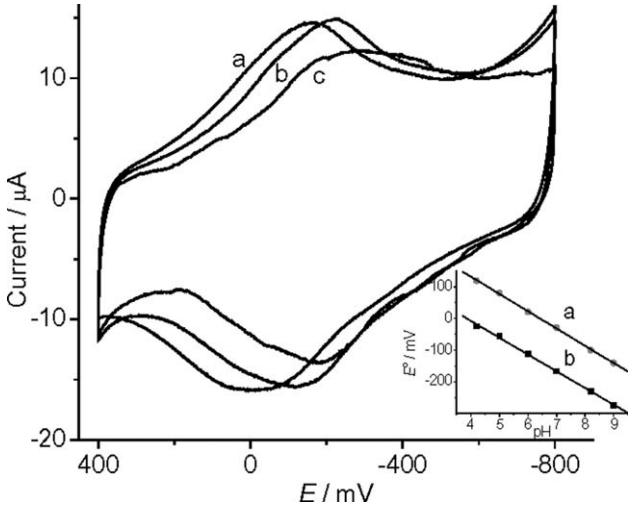

Fig. 5. Cyclic voltammograms of Mb/HMS/GCE in 0.1 M PBS of pH 6.0 (a), pH 7.0 (b), and pH 8.2 (c) at 20 mV/s. Inset: effects of pH on formal potentials of intercalated (a) and adsorbed (b) Mb.

for electron transfer of the immobilized Mb. All changes in voltammetric peak potentials and currents with pH were reversible. For example, the cyclic voltammogram for the Mb/HMS/GCE at pH 9.0 was reproduced after immersion in pH 4.2 buffer and then returned to the pH 9.0 buffer. Plots of the formal potentials of the two couples of redox peaks versus pH (from 4.2 to 9.0) produced two lines with slopes of −52.8 and −54.5 mV/pH, which were close to the expected value of −58.0 mV/pH for a single proton transfer coupled to reversible single electron transfer. The slopes indicated one proton participating in a single electron transfer process [36] for neutralizing the excess charge that accumulated at the interface upon electrochemical reduction. The surface-controlled electrode process indicated that the diffusion of the proton was very fast.

Electrocatalysis of Mb/HMS/GCE to reduction of H_2O_2

Fig. 6 shows typical cyclic voltammetric curves for the H_2O_2 sensor. In 0.1 M, pH 7.0, PBS the cyclic voltammogram of Mb/HMS/GCE shows only the direct electrochemistry. Upon addition of H_2O_2 to the solution, the shape of the cyclic voltammogram for the direct electron transfer of Mb changes dramatically with an increase of reduction current and a decrease of oxidation current, while no electrocatalytic current is observable at a bare GCE or the HMS/GCE (inset in Fig. 6), displaying an obvious electrocatalytic behavior of the Mb intercalated in the mesopores of HMS to the reduction of H_2O_2. With increase of concentration, the cathodic peak potentials shifted to negative value slightly. Thus, the intercalated Mb molecules are of good electrocatalytic activity, and the substrates for enzyme reaction can freely enter the mesopores. Furthermore, the reduction current increases with an increase of H_2O_2 concentration. The electrocatalytic process can be expressed as follows:

$$\mathrm{MbFe(III)} + e \rightarrow \mathrm{MbHFe(II)} \quad (1)$$

$$\mathrm{H_2O_2} + 2\mathrm{MbHFe(II)} \rightarrow 2\mathrm{MbFe(III)} + 2\mathrm{H_2O}. \quad (2)$$

In the presence of H_2O_2, MbHFe(II) was efficiently converted to its oxidized form, MbFe(III). Consequently, more MbFe(III) molecules were reduced at the electrode surface by the direct electron transfer.

The effect of applied potential on the steady state current of the H_2O_2 sensor showed that the electrocatalytic reduction of H_2O_2 could be observed at around −150 mV. With applied potential decreasing from −150 to −400 mV, the steady state current increased due to the increased driving force for the fast reduction of H_2O_2 at the lower potentials. The response approached a plateau value at −400 mV, so we select this value as the working potential for amperometric determinations.

The amperometric response of Mb/HMS/GCE with successive additions of H_2O_2 to 0.1 M, pH 7.0, PBS at an applied potential of−400 mV is shown in Fig. 7. Upon addition of an aliquot of H_2O_2 to the buffer solution, the reduction current increased steeply to reach a stable value. The enzyme electrode achieved 95% of the steady state current in less than 10 s. The results demonstrated clearly that the electrocatalytic response was very fast. With solution pH increasing from 4.2 to 9.0, the amperometric response increased and reached a maximum value at pH 7.0 (Fig. 8). At pH less than 7.0, the increase in amperometric response is attributed to the increase of electrocatalytic activity of Mb. The slight decrease of amperometric response at solution pH of more than 7.0

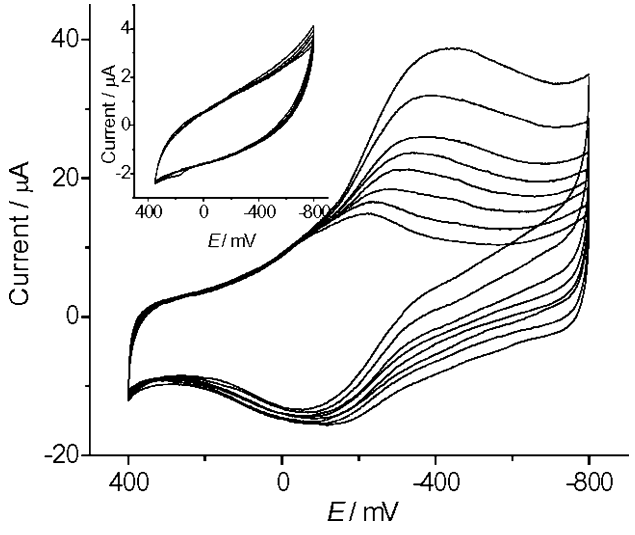

Fig. 6. Cyclic voltammograms of Mb/HMS/GCE in 0.1 M, pH 7.0, PBS containing 0, 0.01, 0.02, 0.03, 0.04, 0.05, 0.07, and 0.09 mM H_2O_2 at 20 mV/s. Inset: cyclic voltammograms of HMS/GCE in 0.1 M, pH 7.0, PBS containing 0, 0.02, 0.04, 0.07, and 0.09 mM H_2O_2 at 20 mV/s.

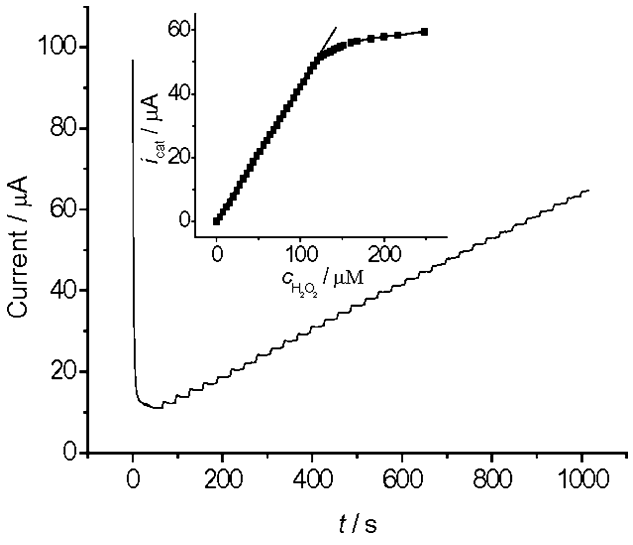

Fig. 7. Amperometric response of the Mb/HMS/GCE at −400 mV upon successive additions of 10 μl 2 mM H_2O_2 to 5.0 ml 0.1 M, pH 7.0, PBS. Inset: plot of catalytic current vs H_2O_2 concentration.

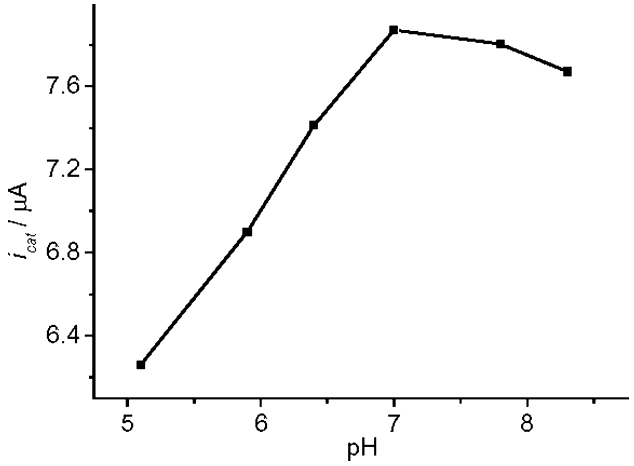

Fig. 8. Effect of pH on amperometric response of Mb/HMS/GCE to 20 μM H_2O_2 in 0.1 M, pH 7.0, PBS.

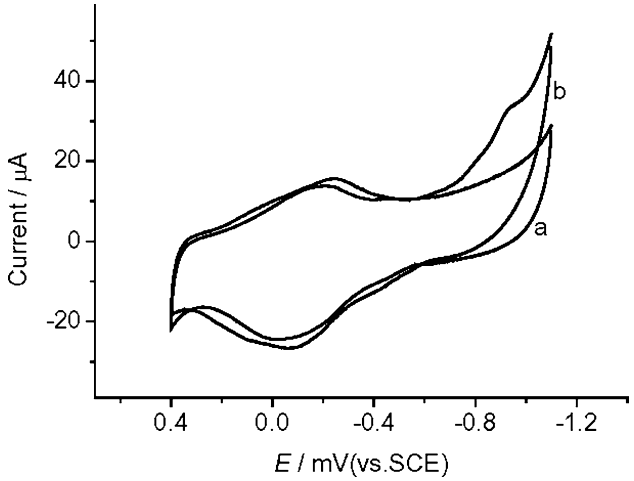

Fig. 9. Cyclic voltammograms of Mb/HMS/GCE in 0.1 M, pH 7.0, PBS containing 0 (a) and 0.1 mM (b) $NaNO_2$ at 20 mV/s.

is due to the denaturing of the immobilized Mb. The response was also related to the charge of zeolite particles on the electrode surface. At low pH, the Mb was a positive-charged molecule, which made it more difficult to approach the positive-charged surface of zeolite particles, producing low current response. Under optimal conditions the linear response range of the sensor to H_2O_2 concentration was from 4.0 to 124 μM with a correlation coefficient of 0.9999 ($n = 32$) (inset in Fig. 7). From the slope of 0.424 μA/μM the detection limit was estimated to be 6.2×10^{-8} M at a signal to noise ratio of 3, which was much lower than that reported for the detection limit of 0.21 μM H_2O_2 [38]. The mean steady state current of 20 μM H_2O_2 for six determinations was 7.85 μA with a RSD of 4.1%.

When the concentration of H_2O_2 was higher than 124 μM, a response platform was observed, showing a characteristic of the Michaelis–Menten kinetic mechanism. The apparent Michaelis–Menten (K_m^{app}) could be obtained from the electrochemical version of the Linweaver–Burk equation [37]. The K_m^{app} value for the electrocatalytic activity of Mb/HMS/GCE to H_2O_2 was determined to be 0.065 ± 0.005 mM which was lower than those of 3.69 mM for HRP/Au/CPE [38], 5.5 mM for membrane-entrapped HRP [39], and 2.3 mM for HRP/Au colloid self-assembled monolayer electrode [40]. Thus, the Mb entrapped in the HMS matrix was of a higher affinity to H_2O_2.

Electrocatalysis of Mb/HMS/GCE to reduction of NO_2^-

Fig. 9 shows the cyclic voltammograms of Mb/HMS/GCE in 0.1 M, pH 7.0, PBS upon addition of $NaNO_2$. A reduction of NO is observed at about −0.96 V. NO is produced from the nitrite disproportionation reaction [41,42]:

$$NO_2^- + 2H^+ + e^- \rightarrow NO + H_2O. \quad (3)$$

Thus −1.0 V was applied to amperometric detection of NO_2^-.

Fig. 10 shows the amperometric response of the Mb/HMS/GCE with successive additions of $NaNO_2$ to 0.1 M, pH 7.0, PBS at an applied potential of −1000 mV. No response is observable at the HMS/GCE. This reaction and the uneven concentration of NO_2^- on the electrode surface when new NO_2^- solution was added into the buffer resulted in the current decrease over time. After a reaction time of 30 s the current was stable and reproducible. Upon addition of an aliquot of $NaNO_2$ to the buffer, the reduction current of NO_2^- increases steeply, indicating a fast reduction rate. With an increase of $NaNO_2$ concentration, the amperometric response increases. Inset in Fig. 10 shows the calibration curve of the Mb/HMS/GCE to $NaNO_2$. The linear response

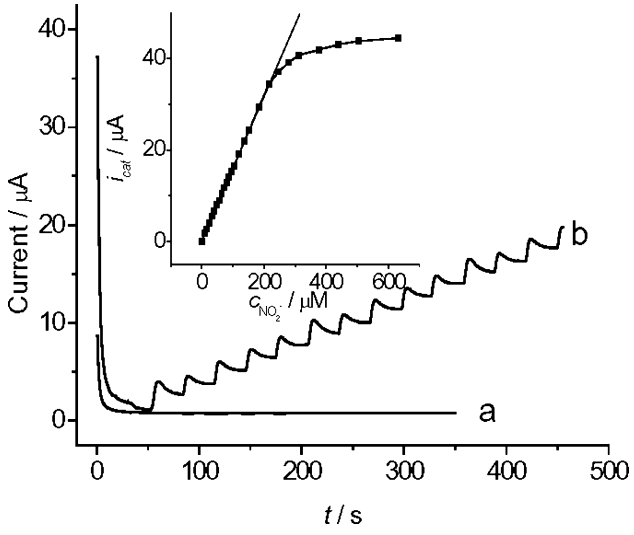

Fig. 10. Amperometric response of the HMS/GCE (a) and Mb/HMS/GCE (b) at –1000 mV upon successive additions of 20 μl 2 mM $NaNO_2$ to 5.0 ml, pH 7.0, PBS. Inset: plot of catalytic current vs $NaNO_2$ concentration.

range of the sensor to NO_2^- concentration is from 8.0 to 216 μM with a correlation coefficient of 0.9999 ($n = 19$). From the slope of 0.158 μA/μM, a detection limit of 8.0×10^{-7} M was obtained at a signal to noise ratio of 3, which was much lower than that reported for the detection limit of 0.1 mM NO_2^- [43]. At 40 μM $NaNO_2$ concentration, the mean steady state current for six determinations was 6.68 μA with a RSD of 3.8%. At NO_2^- concentrations higher than 216 μM, the calibration curve showed a platform. The K_m^{app} value of the Mb/HMS/GCE to $NaNO_2$ was estimated to be 0.72 mM, indicating a high affinity of the Mb/HMS/GCE to NO_2^-.

Effect of temperature on the H_2O_2 and NO_2^- sensors

Temperature is an important parameter affecting the electrocatalytic activity of enzyme or protein. Fig. 11 shows the effect of temperature on amperometric responses. With temperature increasing from 15 to 40 °C, the amperometric responses and the electrocatalytic activities of the immobilized Mb to H_2O_2 and NO_2^- increase. The Mb has activity even at 60 °C. It is evident that the immobilized Mb has good thermal stability because of the unchangeability of microenvironment and its native structure upon temperature change. These results indicate that the sensors can handle a wide range of temperature.

Stability and reproducibility of the H_2O_2 and NO_2^- sensors

The direct electrochemistry of the Mb/HMS/GCE could retain constant current values upon continuous cyclic sweep over the potential range from −0.8 to 0.4 V at 20 mV/s. The immobilized Mb/HMS/GCE lost only

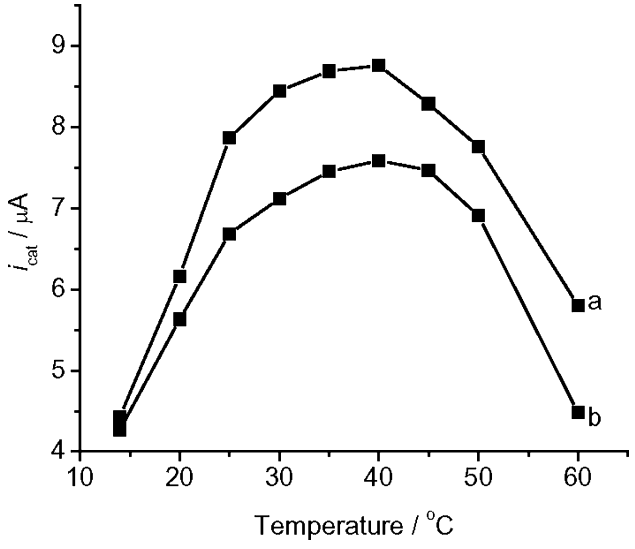

Fig. 11. Effects of temperature on amperometric responses of 20 μM H_2O_2 (a) and 40 μM $NaNO_2$ (b) in 0.1 M, pH 7.0, PBS.

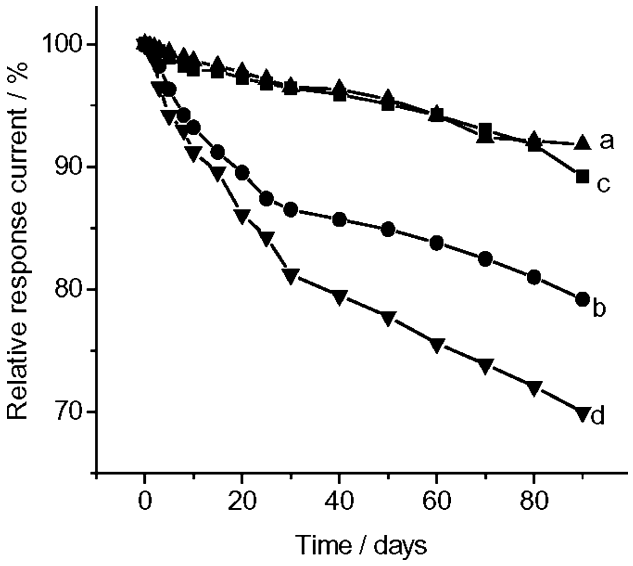

Fig. 12. Stability of the biosensors for H_2O_2 (a,b) and NO_2^- (c,d) stored in 0.1 M, pH 7.0, PBS (a,c) and in air (b,d) at 4 °C.

8.1% of its initial activity after more than 300 successive measurements.

The fabrication of 10 electrodes, made independently, showed an acceptable reproducibility with a RSD of 4.2% for the current determined at a H_2O_2 concentration of 20 μM and 5.2% at a $NaNO_2$ concentration of 40 μM. Thus, HMS particles were very efficient in retaining the electrocatalytic activity of Mb and preventing it from leaking out of the sensor.

In addition to good reproducibility, HMS membrane imparted H_2O_2 and NO_2^- biosensors a good long-term stability. The storage stabilities of H_2O_2 and NO_2^- biosensors stored in 0.1 M, pH 7.0, PBS or air at 4 °C were examined by checking periodically their relative response currents (the ratios of the catalytic currents detected at different times to the initial current value) in 0.1 M, pH 7.0, PBS containing 20 μM H_2O_2 and 40 μM $NaNO_2$, respectively (Fig. 12). The sensors retained 95% of activity to both H_2O_2 and NO_2^- within a storage period of 52 days in 0.1 M, pH 7.0, PBS at 4 °C, while only 84.5 and 77.3% of activity to H_2O_2 and NO_2^- were retained when stored in air at 4 °C, respectively. After a storage period of 3 months in 0.1 M, pH 7.0, PBS at 4 °C, the biosensor showed an 8% loss of activity for H_2O_2 and 11% loss of activity for NO_2^-. Thus, the biosensors were stored in 0.1 M, pH 7.0, PBS at 4 °C, when not in use.

Conclusions

Myoglobin can act within the specific sites on the inner wall of hexagonal mesoporous silica. The larger total specific area of the pores of the molecular sieves compared to that of its surface allows more Mb to

intercalate in the pores. Both the Mb adsorbed on the surface and that intercalated in the mesopores show a good direct electrochemistry, which can be distinguished with their formal potentials. The uniform porous structure of HMS provides a microenvironment around the protein to retain the electrocatalytic activity. The immobilized Mb displays a high affinity and high response sensitivity to both hydrogen peroxide and nitrite without the aid of any electron mediator. The sensor shows a good reproducibility and stability. HMS provides an efficient strategy and a new promising platform for the study of electron transfer of proteins and the development of biosensors.

Acknowledgments

We gratefully acknowledge the financial support of the Distinguished Young Scholar Fund to HX Ju (20325518), the National Natural Science Foundation of China (20275017 and 90206037), the Specialized Research Fund for the Excellent Young Teachers from Ministry of Education of China, and the Science Foundation of Jiangsu (BS2001063).

References

[1] E.D. Bowden, F.M. Hawkridge, H.N. Blount, Bioelectrochemistry, in: S. Srinivasan, Y.A. Chizmadzhev, J.O.'M. Bockris, B.E. Conway, E. Yeager (Eds.), Coprehensive treatise of electrochemistry, Plenum Press, New York, 1985, p. 297.

[2] J.F. Stargardt, F.M. Hawkridge, H.L. Landrum, Reversible heterogeneous reduction and oxidation of sperm whale myoglobin at a surface modified gold minigrid electrode, Anal. Chem. 50 (1978) 930–932.

[3] I. Taniguchi, K. Watanabe, M. Tominaga, F.M. Hawkridge, Direct electron transfer of horse heart myoglobin at an indium oxide electrode, J. Electroanal. Chem. 333 (1992) 331–338.

[4] M. Tominaga, T. Kumagai, S. Takita, I. Taniguchi, Effect of surface hydrophilicity of an indium-oxide electrode on direct electron transfer of myoglobin, Chem. Lett. (1993) 1771–1774.

[5] K. Chattopadhyay, S. Mazumdar, Direct electrochemistry of heme protein: effect of electrode surface modification by neutral surfactants, Bioelectrochemistry 53 (2000) 17–24.

[6] B.C. King, F.M. Hawkridge, A study of the electron transfer and oxygen binding reaction of myoglobin, J. Electroanal. Chem. 237 (1987) 81–92.

[7] I. Hamachi, N. Shunsaku, T. Kunitake, Functional conversion of myoglobin bound to synthetic bilayer membranes: from dioxygen storage protein to redox enzyme, J. Am. Chem. Soc. 113 (1991) 9625–9630.

[8] J.F. Rusling, A-E.F. Nassar, Enhanced electron-transfer for myoglobin in surfatant films on electrodes, J. Am. Chem. Soc. 115 (1993) 11891–11897.

[9] A-E.F. Nassar, W.S. Willis, J.F. Rusling, Electron transfer from electrodes to myoglobin: facilitated in surfactant films and blocked by adsorbed biomacromolecules, Anal. Chem. 67 (1995) 2386–2392.

[10] Y. Okahata, G. Enna, K. Taguchi, T. Seki, Electrochemical permeability control through a bilayer-immobilized film containing redox sites, J. Am. Chem. Soc. 107 (1985) 5300–5301.

[11] Y. Okahata, G. Enna, Permeability controllable membranes. Electrochemical responsive gate membranes of multiplayer film containing a viologen group as redox sites, J. Phys. Chem. 92 (1988) 4546–4551.

[12] J.F. Rusling, Enzyme bioelectrochemistry in cast biomembrane like films, Acc. Chem. Res. 31 (1998) 363–369.

[13] D. Mimica, J.H. Zagal, F. Bedioui, Electroreduction of nitrite by hemin, myoglobin and hemoglobin in surfactant films, J. Electroanal. Chem. 497 (2001) 106–113.

[14] A.-E.F. Nassar, Z. Zhang, N. Hu, J.F. Rusling, T.F. Kumosinski, Proton-coupled electron transfer from electrodes to myoglobin in ordered biomembrane-like films, J. Phys. Chem. 101 (1997) 2224–2231.

[15] A.-E.F. Nassar, J.M. Bobbitt, J.D. Stuart, J.F. Rusling, Catalytic reduction of organhalide pollutants by myoglobin in a biomembrane-like film, J. Am. Chem. Soc. 117 (1995) 10986–10993.

[16] T.K. Das, S. Mazumdar, S. Mitra, Micelle induced release of heme NO from nitrite oxide complex of myoglobin, J. Chem. Soc. Chem. Commun. (1993) 1447–1448.

[17] C. Lei, F. Lisdat, U. Wollenberger, F.W. Scheller, Cytochrome c/clay-modified electrode, Electroanalysis 11 (1999) 274–276.

[18] C. Lei, J. Deng, Hydrogen peroxide sensor based on coimmobilized methylene green and horseradish peroxidase in the same montmorillonite-modified bovine serum albumin-glutaraldehyde matrix on glassy carbon electrode surface, Anal. Chem. 68 (1996) 3344–3349.

[19] C. Fan, Y. Zhuang, G. Li, J. Zhu, D. Zhu, Direct electrochemistry and enhanced activity for hemoglobin in a sodium montmorillonit film, Electroanalysis 12 (2000) 1156–1157.

[20] Y. Sallez, P. Bianco, E. Lojou, Electrochemical behavior of c-type cytochromes at clay-modified carbon electrodes: a model for the interaction between proteins and soils, J. Electroanal. Chem. 493 (2000) 37–49.

[21] O. Ikeda, M. Ohtani, T. Yamaguchi, A. Komura, Direct electrochemistry of cytochrome c at glassy carbon electrode covered with a microporous alumina membrane, Electrochim. Acta 43 (1998) 833–839.

[22] J. Yu, H. Ju, Preparation of porous titania sol-gel matrix for immobilization of horseradish peroxidase by a vapor deposition method, Anal. Chem. 74 (2002) 3579–3583.

[23] P. Rolison, Zoelite-modified electrodes and electrode-modified zeolites, Chem. Rev. 90 (1990) 867–878.

[24] P.T. Tanev, M. Chibwe, T.J. Pinnavaia, Titanium-containing mesoporous molecular sieves for catalytic oxidation of aromatic compounds, Nature 368 (1994) 321–323.

[25] E.P. Barrett, L.G. Joyner, P.H. Halenda, The determination of pore volume and area distributions in porous substance, Computations from nitrogen isotherms, J. Am. Chem. Soc. 73 (1951) 373–380.

[26] M.W. Anderson, J. Klinowski, Zeolites treated with silicon tetrachloride vapor. Part¢ñ preparation and characterization, J. Chem. Soc. Faraday Trans. 1 (82) (1986) 1449–1469.

[27] J.K Kauppinen, D.J. Moffatt, H.H. Mantsch, D.G. Cameron, Resolution of complex band contours by means of Fourier self-deconvolution, Appl. Spectrosc. 35 (1981) 271–276.

[28] B. Liu, R. Hu, J. Deng, Characterization of immobilization of an enzyme in a modified Y zeolite matrix and its application to an amperometric glucose biosensor, Anal. Chem. 69 (1997) 2343–2346.

[29] J.F. Diaz, K.J. Balkus Jr., Enzyme immobilization in MCM-41 molecular sieve, Mol. Catal. B: Enzymatic. 2 (1996) 115–126.

[30] H. Takahashi, B. Li, T. Sasaki, C. Miyazaki, T. Kajino, S. Inagaki, Immobilized enzymes in ordered mesoporous silica materials and improvement of their stability and catalytic activity in an organic solvent, Micro. Meso. Mater. 45 (2001) 755–762.

[31] P.T. Tanev, T.J. Pinnavaia, Recent advances in synthesis and catalytic applications of mesoporous molecular sieves, Access Nanoporous Mater. (Proc. Symp.) (1995) 13–27.

[32] R.W. Murray, in: A.J. Bard (Ed.), Electroanalytical Chemistry, vol.13, Marcel Dekker, New York, 1984, pp. 191–368.
[33] Y. Hu, N. Hu, Y. Zeng, Facilitated electron transfer for myoglobin in surfactant polymer $2C_{12}N^{+}PVS^{-}$ composite films on pyrolytic graphite electrodes, Microchem. J. 65 (2000) 147–157.
[34] H.M. Zhang, N.Q. Li, The direct electrochemistry of myoglobin at a DL-homocysteine self-assembled gold electrode, Bioelectrochem. Bioenerg. 53 (2000) 97–101.
[35] A.L. Lehninger, Biochemistry: The molecular basic of cell structure and function, second ed., Worth Publisher, 1975, Chap. 7.
[36] A.M. Bond, Modern polarographic methods in analytical chemistry, Marcel Deckker, New York, 1980, 27.
[37] R.A. Kamin, G.S. Willson, Rotating ring-disk enzyme electrode for biocatalysis kinetic studies and characterization of the immobilized enzyme layer, Anal. Chem. 52 (1980) 1198–1205.
[38] S.Q. Liu, H.X. Ju, Renewable reagentless hydrogen peroxide sensor based on direct electron transfer of horseradish peroxidase immobilized on colloidal gold-modified electrode, Anal. Biochem. 307 (2002) 110–116.
[39] T. Ferri, A. Poscia, R. Santucci, Direct electrochemistry of membrane-entrapped horseradish peroxidase. Part II: Amperometric detection of hydrogen peroxide, Bioelectrochem. Bioenerg. 45 (1998) 221–226.
[40] Y. Xiao, H.X. Ju, H.Y. Chen, Direct electrochemistry of horseradish peroxidase immobilized on a colloidal/cysteamine-modified gold electrode, Anal. Biochem. 278 (2000) 22–28.
[41] M.H. Barley, K.J. Takcuchi, T.J. Meyer, Electrocatalytic reduction of nitrite to ammonia based on a water-soluble iron porphyrin, J. Am. Chem. Soc. 108 (1986) 5876–5885.
[42] J.N. Younathan, K.S. Wood, T.J. Meyer, Electrocatalytic reduction of nitrite and nitrosyl by iron protoporphyrin dimethyl ester immobilized in an electropolymerized film, Inorg. Chem. 31 (1992) 3280–3285.
[43] L. Shen, R. Huang, N. Hu, Myoglobin in polyacrylamide hydrogel films:direct electrochemistry and electrochemical catalysis, Talanta 56 (2002) 1131–1139.